

# **Influence of Gravity Framing on the Collapse Probability of Steel Buildings with Special Moment Frames**

**Adem KARASU<sup>1</sup>**

**Cüneyt VATANSEVER<sup>2</sup>**

## **ABSTRACT**

This paper presents the influence of gravity framing on the collapse risk of steel frame buildings with perimeter special moment frames (SMFs) designed in Turkey. For this, four- and eight-story buildings have been designed considering the related current specifications and codes. Header end-plate connections are used for the beam-to-column joints of the gravity frame system. A nonlinear analytical model that simulates the hysteretic behavior of header end-plate connections is calibrated with past experimental data. Nonlinear static pushover analysis (NSPA) and nonlinear response history analyses (NRHAs) were implemented for both four-story and eight-story SMFs with and without the gravity framing to quantify their collapse performance and monitor the system-level seismic response of the building through collapse. The advantage of presence of the gravity framing is investigated and differences in structural responses between the models are also examined. When the models were excited by different ground motions, median responses of the detailed models showed an increase in lateral force carrying capacity and a decrease in first-story drift demand, compared to the nonlinear static pushover analyses results. Furthermore, the results demonstrate that gravity frames in a structure profoundly decrease the possibility of collapse.

**Keywords:** Steel structures, gravity framing, nonlinear dynamic analysis, collapse probability.

## **1. INTRODUCTION**

Before the Northridge earthquake, welded moment resisting frames had been considered to be the most ideal structural system. Following the Northridge Earthquake many steel moment resisting frames experienced fractures in the beam-to-column joints. The damage observed after the earthquake ranged from minor cracking to completely severed members. However, structural collapse was not observed after the Northridge earthquake. The most likely reason

---

Note:

- This paper has been received on October 12, 2020 and accepted for publication by the Editorial Board on January 18, 2021.
- Discussions on this paper will be accepted by September 30, 2022.

• <https://doi.org/10.18400/tekderg.809233>

1 Istanbul Technical University, Department of Civil Engineering, Istanbul, Turkey - [karasud@itu.edu.tr](mailto:karasud@itu.edu.tr) - <https://orcid.org/0000-0002-1063-8484>

2 Istanbul Technical University, Department of Civil Engineering, Istanbul, Turkey - [cuneyt.vatansever@itu.edu.tr](mailto:cuneyt.vatansever@itu.edu.tr) - <https://orcid.org/0000-0002-9954-925X>

that the buildings remained standing is that the gravity framing acted as a “backup system” preventing structural collapse (Leon [1]). The damage observed after the Northridge Earthquake exposed weakness of design procedures and led to the development of performance-based guidelines. Furthermore, performance assessment by nonlinear dynamic analyses is increasingly used for the seismic assessment of buildings.

Over decades, various research projects have focused on predicting seismic collapse capacity of structural systems (Huang and Foutch [2], Lignos and Krawinkler [3]). Gupta and Krawinkler [4] affirmed that the gravity system can significantly increase the post-yield stiffness of the structure which in turn reduces the influence of P-Delta effects under high intensity ground motions. According to their study, the gravity frames could be effective in delaying or preventing dynamic instability if the gravity framing increases the post-yield tangent stiffness. Ramos et al. [5] presented a series of hybrid simulations conducted on a four-story steel moment frame to experimentally assess the seismic performance of a steel building from the onset of damage through collapse. MacRae et al. [6] showed that the continuous gravity column in a structure significantly decrease the possibility of large drift concentrations and prevent soft story mechanism for braced frames. Ji et al. [7] demonstrated that gravity columns can contribute to the mitigation of drift concentration by adding lateral stiffness and strength for multi-story concentrically braced frames. Elkady and Lignos [8] showed that when the contribution of the gravity framing is considered, total base shear strength of steel buildings with steel SMFs is on average 50% larger than bare frame and this was primarily attributed to the gravity framing as well as the composite action provided by the concrete slab. Lee and Foutch [9] evaluated performance of the post-Northridge buildings and showed that they have a high confidence level of satisfying collapse prevention and immediate occupancy performance objectives. Flores et al. [10] investigated the influence of the gravity framing system on the seismic performance of SMFs and concluded that continuous stiffness provided by gravity column with no splices helps the structure deform in the first mode and that is why drift concentrations and soft story mechanisms could be prevented. Foutch and Yun [11] showed that when the gravity framing system is considered as a part of the corresponding analytical model, its lateral stiffness and strength are increased and story drift concentrations along the height of a steel frame building can be mitigated. Astaneh-Asl et al. [12] assessed the seismic performance of moment resisting frames damaged during the Northridge earthquake and concluded that, for buildings subjected to Northridge-Newhall records, the roof drift and base shear of the damaged semi-rigid frame is smaller than the roof drift of the undamaged rigid frame. Sizemore et al. [13] performed nonlinear inelastic analysis as well as nonlinear inelastic incremental dynamic analysis for suite of earthquake ground motions. The results showed that the fixity of the bases in the gravity framing system appears to be very effective at providing reserve strength and stiffness to the system, which helps to prevent collapse for concentrically braced frames.

Secondary systems such as the gravity framing system are typically ignored in seismic performance assessment of structures. The simple connections such as header end-plate connections that may be used in gravity frames are assumed to provide minimal lateral resistance to the structure. However, quasi-static experimental tests show that header end-plate connections have some inherent flexural capacity reaching up to 34% of the plastic flexural capacity  $M_p$ , of the gravity beam with increasing strength and stiffness at large displacements (Karasu and Vatansever [14]).

Limited research has been conducted to assess the effect of the gravity framing system on the seismic response of structures near collapse. Considering the large number of beam-to-column joints which are nominally defined as pinned connections such as header end-plate connections, their contribution to its lateral load resistance may be significantly larger than expected. In addition, the considerable flexural capacity of header end-plate connections in conjunction with the gravity column is assumed to behave as a secondary lateral load resisting system. As a result, it could possibly help to share the story shear force which in turn relieve the existing seismic force resisting frames from excessive story shear.

In most of the studies conducted, beam-to-column connections of the interior gravity frames are typically designed with shear tab connections. The motivation for the study presented here was the lack of studies where the header end-plate beam-to-column connections are used as the connections of gravity frames.

In this paper, two types of buildings with four and eight stories were designed in accordance with the Turkish Seismic Code for Buildings 2018 (TSCB 2018, [15]). The influence of the gravity frames on the seismic response of steel buildings that utilize perimeter special moment frames is traced from the onset of damage through collapse. The effect of the gravity frames on the steel building's over-strength and collapse capacity is investigated. Only side-sway collapse mechanisms are considered in the present study, where dynamic instability results from second-order P-Delta effects accelerated by component deterioration fully overcoming the shear resistance of a structure at large lateral deformations.

## **2. BEAM-TO-COLUMN CONNECTIONS IN GRAVITY FRAMES**

Accurate response predictions of steel buildings subjected to earthquake loading involve the use of models which are able to simulate properly the cyclic behavior of the critical regions such as beam-to-column connections. In this study, calibration conducted to better represent the behavior of the header end-plate beam-to-column connections is based on matching the numerical cyclic model and experimental data retrieved from Karasu and Vatansever [14]. Furthermore, the calibrated models should be able to represent hardening and softening, stiffness and strength degradation properties of the moment-rotation curve of the connection. However, according to the main outcome from the study given (Chisari et al. [16]) is that a calibration based on cyclic response only is not robust, because under different loading conditions, its accuracy may deteriorate. Nevertheless, steel gravity framing connection models are required for detailed structural analysis at the macro level.

This section discusses the approach used to explicitly model the cyclic behavior of bare header end-plate connections as a part of gravity frame. The ductile behavior of header end-plate connections generally governed by the flexural behavior of end-plate and eventually connection failure as a result of end-plate tearing at large rotations. Experimental test results for specimens T4-15 and T5-15 (Karasu and Vatansever [14]) showed that symmetric cyclic behavior was observed in both positive and negative moments. Since composite action between the beam and concrete slab was ignored in the tests, the maximum moment was taken 34% of the plastic flexural capacity  $M_p$ , of the gravity beam at both side of the moment-rotation curve. The 'UniaxialMaterial Hysteretic' material model available in OpenSees [17] was employed to simulate the actual behavior of the beam-to-column connections with header end-plates under cyclic loading. The model simulates moment-rotation curve of a

structural component that exhibits degradation in flexural strength and stiffness under cyclic loading. The cyclic deterioration in unloading stiffness is controlled with beta parameter. The pinching of force and deformation, damage due to ductility and energy are controlled with the parameters of pinchY, pinchX, damage1 and damage2, respectively. Table 1 summarizes the cyclic deterioration parameters for header end-plate connections. Figure 1 shows the calibrated examples of hysteretic material models with experimental data (Karasu and Vatansever [14]). The calibrated hysteretic model shown in Fig. 1 is assumed to be acceptable to represent the behavior of the gravity framing connections. Beyond the maximum rotations given in Figure 1, calibrated hysteretic models do not deteriorate further according to program algorithm. This condition is consistent with the behavior of specimen T4-15 in which larger rotations can be maintained without loss of strength.

*Table 1 – Calibrated cyclic deterioration parameters of the hysteretic material model for the specimens of T4-15 and T5-15*

	pinchX	pinchY	damage1	damage2	beta
T4-15	0.55	0.60	0	0	0.4
T5-15					

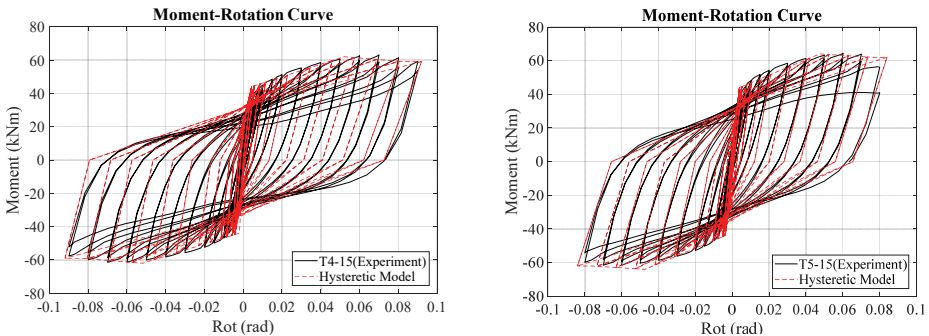


*Figure 1 - Comparison of the hysteretic models and experimental test results*

### **3. BUILDING OVERVIEW**

In this study, to evaluate the effect of the gravity framing on the seismic response of steel buildings with perimeter SMFs, two typical steel buildings with different heights of 4 and 8 stories are designed with current specifications and codes in Turkey such as Turkish Seismic Code for Buildings 2018 (TSCB 2018, [15]) and Turkish Code for Design and Construction of Steel Structures (TCDCSS 2016, [18]). Simple elastic models based on centerline dimensions of beams and columns were used for the design of steel buildings. This method has been found acceptable for design of SMFs (Krawinkler [19]). Direct analysis method was used to obtain the required strengths including second order effects for the structural members. For this, 3D structural model of the buildings has been developed and analyses have been performed by using SAP2000 software [20]. In design, the equivalent lateral force method was employed for the distribution of the seismic base shears on the structural systems. The lateral force resisting system of the buildings consists of special moment frames

with reduced beam section in both principle directions resulting in the response reduction factor of  $R=8$ . Reduced beam section connection model was built by reducing the beam flange area to form plastic hinges away from column face.

Figure 2 and Figure 3 illustrate a typical plan and elevations of the steel buildings including assigned member sections as a result of the analyses, respectively. The plan view of the steel buildings is selected similar to the archetype steel frame buildings described in [8]. This plan view is considered to be feasible in order to better explain and conveniently model the gravity frames. The filled triangle represents moment resisting connections (MC) and hollow circle represents pin connections (PC) for the simple model as shown in Figure 2. The buildings were assumed to locate in Istanbul. Design spectral acceleration at the short period,  $S_{DS}$  and at a period of 1 second  $S_{D1}$  are equal to  $0.873g$  and  $0.451g$  respectively and the soil conditions were assumed to be defined as soil type ZD and this corresponds to seismic design category 1 in Turkish Seismic Code for Buildings 2018 (TSCB 2018, [15]). The buildings have a ground-story height of 4.0 m and a typical story height of 3.0 m. The bay width between columns is 6.0 m. The dead load is  $4.9 \text{ kN/m}^2$  on all floors and  $4.0 \text{ kN/m}^2$  on the roof. The unreduced live load is  $2.0 \text{ kN/m}^2$  uniformly distributed over each floor. Wind load was not considered as a part of the design process. The beams and columns are fabricated from European steel sections with a specified minimum yield stress  $F_y=275 \text{ N/mm}^2$  (S275). The interior gravity framing system of the buildings consists of 16 gravity columns and 40 gravity beams at each floor. The gravity columns are oriented around their strong axis with respect to East-West loading direction and considered as a pin connected at the base. The gravity columns and beams are assigned HE300B and IPE300 sections, respectively. In the gravity frames, the same column section is used to reflect the experimental study [14] through the height of the two buildings. The interior gravity framing connections are designed as header end-plate connections. The column bases were considered as fixed at the base of the SMFs.

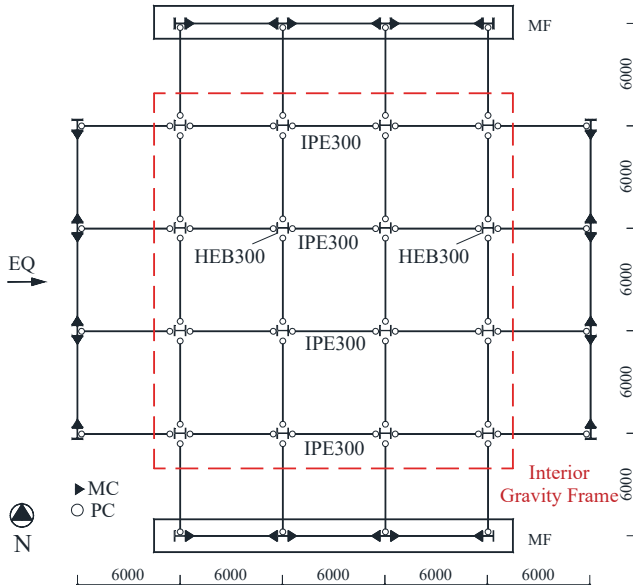


Figure 2 - Plan view of typical steel buildings with SMFs



the inelastic behavior of the plastic hinges located at the reduced beam section and the actual behavior of header end-plate connections for SMFs and equivalent gravity frame, respectively. Column springs represent the potential plastic hinges at the extremes of columns for both SMFs and equivalent gravity frame. These springs are able to capture the cyclic deterioration in flexural strength and stiffness of steel components subjected to cyclic loading. These hysteretic models are called modified Ibarra-Medina-Krawinkler (IMK) deterioration model. The input parameters of the IMK deterioration model can be computed from multivariate regression equations developed by Lignos and Krawinkler [22] and Lignos et al. [23]. The panel zones were explicitly modeled using the parallelogram model (Gupta and Krawinkler [24]). The inelastic behavior of the panel zone is captured with a tri-linear hysteretic model.

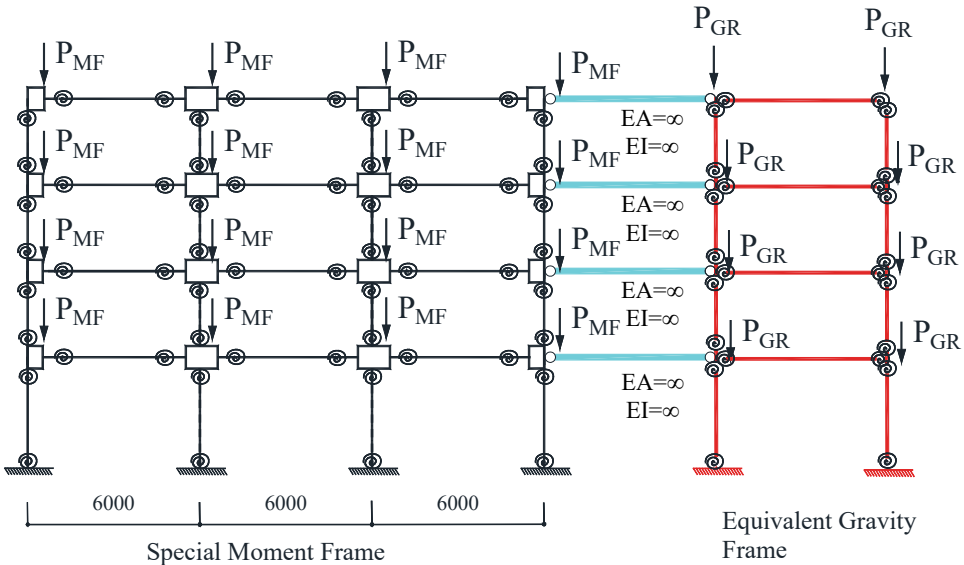


Figure 4 - 2D OpenSees model of the SMFs including equivalent gravity frame

A fictitious single-bay frame is attached to the main SMF using axially rigid trusses, as indicated by Gupta and Krawinkler [24] and Lignos et al. [25] to account for the gravity framing as part of 2D analytical model representations of the same steel building in its East-West loading direction. This frame is called the equivalent gravity frame that may be represented with a single-bay in case of rigid diaphragm assumption. In order to lump together n-bay frames into a single-bay frame with an equivalent beam length  $L_{b,eq}$ , moment of inertia  $I_{b,eq}$ , plastic moment  $M_{p,b,eq}$  and equivalent columns with moment of inertia  $I_{c,eq}$ , and plastic moment  $M_{p,c,eq}$  the following rules apply;

$$\sum_{n=1}^n EI_{b,i} / L_{b,i} = EI_{b,eq} / L_{b,eq}, \quad \sum_{n=1}^n EI_{c,i} = 2EI_{c,eq} \quad (1)$$

$$\sum_{n=1}^n M_{pb,i} = M_{pb,eq}, \quad \sum_{n=1}^n M_{pc,i} = 2M_{pc,eq} \tag{2}$$

In the equations given above, E is the modulus of elasticity of the steel material,  $I_{b,i}$ ,  $L_{b,i}$  and  $M_{pb,i}$  are the moment of inertia, length and plastic moment of i-th beam in a story, respectively,  $I_{c,i}$  and  $M_{pc,i}$  are the moments of inertia and plastic moment of i-th column in a story, respectively. For example, the elastic element of the equivalent gravity frame beam in i-th story is assigned a flexural strength and stiffness equal to half of the sum of those gravity beams (ten gravity beams) in i-th story for the East-West direction.

The P-Delta load equal to half of the gravity load ( $1.05G + 0.25Q$  [26]) of the building minus the tributary load that is assigned to the SMFs columns is divided equally and applied to the columns of the equivalent gravity frame. Geometric nonlinearities are captured using the simplified P-Delta formulation available in OpenSees. Doubler plates were inserted at the panel zones of the interior SMF columns to satisfy the shear requirement. Steel SMFs are designed with strong column/weak beam ratios larger than 1.0. Rayleigh damping is incorporated to in the 2D models. The stiffness-proportional term is assigned to elastic beam and column elements while the mass-proportional term is assigned to all the frame nodes. Two percent Rayleigh damping ratio is assigned at the first and third mode of all buildings according to approach given in the studies ([Zareian and Medina [27] and Chopra [28]). Based on the eigenvalue analysis, the first mode periods of the model BF and Model GF are summarized in Table 2.

*Table 2 - First mode periods of the models*

T <sub>1</sub> (s)	4-Story		8-Story	
	Model BF	Model GF	Model BF	Model GF
SAP 2000 3D Model	0.92	-	1.50	-
OpenSees 2D Model	0.86	0.82	1.32	1.28
Empirical Equation [15]	0.767	0.767	1.25	1.25

As a result of the eigenvalue analyses, GF Models are stiffer than the bare BF models. This is indicated by the smaller periods of GF models compared to BF models. This difference is attributed to the gravity framing effect. Moreover, while simple 3D models use centerline dimensions and panel zones without doubler plates, 2D models use clear length and stronger panel zone with doubler plates. That leads to differences between the first mode period of the 3D and 2D models. The differences between the first mode period of the 3D and 2D models are minimized when both ignoring the doubler plates inserted at the panel zone of the SMF columns and using centerline dimensions of beams and columns in the 2D models. Therefore, OpenSees models are found to be acceptable to represent the nonlinear behavior of 3D building model in East-West direction.

## 5. NONLINEAR STATIC PUSHOVER ANALYSIS

The nonlinear static pushover analysis (NSPA) has much value in understanding significant characteristics that are not being explored in a nonlinear response history analysis (NRHA). In a pushover analysis, engineers generally focus on the demand/capacity ratio rather than visualization of the building behavior. Therefore, it is proposed to employ a combination of NSPA and NRHAs to understand the seismic performance of steel buildings with SMFs (Lignos et al. [25] and Lignos et al. [29]). In the present study, 2D detailed OpenSees models were adopted to conduct both nonlinear static pushover and nonlinear response history analyses.

The nonlinear static pushover analysis was performed on each building to evaluate gravity framing effect on the static over-strength of the steel buildings. Pushover analysis is conducted using the first-mode lateral load pattern for each steel building in the East-West direction. The force and displacement relationships were plotted in terms of the seismic base shear and roof drift. The roof drift is calculated by dividing the roof displacement by the total height of the building. The over-strength ratio  $D$ , was defined here as the ratio of ultimate strength  $V_{max}$  of the frame to the design strength  $V_{des}$ , given in TSCB 2018, [15]. Table 3 summarizes the over-strength ratio obtained for all of the buildings with steel SMFs. The static over-strength factors ( $D$ ) obtained from analyses are much higher than given in the code ( $D=3$ , Table 4.1) (TSCB 2018, [15]). Because the strict rule on inter-story drift limits based on the equivalent displacement approach makes the structure extremely stiff and that leads to larger member sections. For example, in design, deflection amplifier factor was taken to be equal to  $R/I=8/1=8$  (Response modification factor/Importance factor) according to TSCB 2018 [15], that is larger value comparing to the value of  $C_d/I=5.5/1=5.5$  as specified in ASCE provisions (ASCE/SEI 2017, [30]). In conclusion, drift requirements governed the design for both of the buildings, and demand/capacity ratios in terms of the strength were very low at the end of the analyses.

Table 3 - Over-strength factors ( $D$ ) obtained from NSPA analysis

	4-Story		8-Story	
	Model BF	Model GF	Model BF	Model GF
$V_{max}$ (kN)	6039.65	7158.92	8679.40	9614.17
$V_{des}$ (kN)	1172.45	1172.45	1466.94	1466.94
$D$	5.15	6.10	5.91	6.55
Model GF / Model BF	1.185		1.108	

Analysis results, shown in Figure 5, demonstrate the benefits of the interior gravity frames on the secondary stiffness and lateral load carrying capacity. The four-story building experiences more than 18% increase in base shear strength compared with 10.8% for eight-story as a result of the consideration of the gravity framing. The higher effect of P-Delta is noticeable for the eight-story building because pushover curves of the eight story models shows steeper negative tangent slopes at larger drifts due to stiffness and strength deterioration of the structural components.

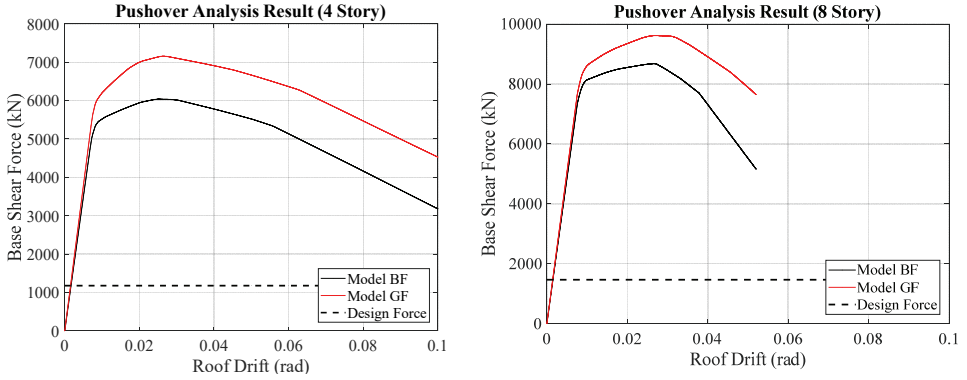


Figure 5 - Pushover curves of steel buildings

Once the global strength deterioration occurs, the period based ductility  $\mu_T$  is indicator of the buildings performance. In FEMA P695 [26], this factor is defined as the ratio of the global roof drift to corresponding to a 20% drop in the maximum base shear to global yield roof drift. As shown in Figure 5, GF models achieve larger  $\mu_T$  values. This is attributed to the smoother post-capping stiffness of the GF models. Because when the gravity framing is considered as a part of the lateral force resisting system of the building; there is less drift concentration in the bottom stories of the steel buildings especially for the eight-story steel building. In general, a four-story collapse mechanism is developed compared to the three-story one of the bare BF model for the eight-story building and more energy is dissipated through the beams of the SMFs that contribute to larger lateral load carrying capability. In Figure 6, red filled circles represent plastic hinge regions.

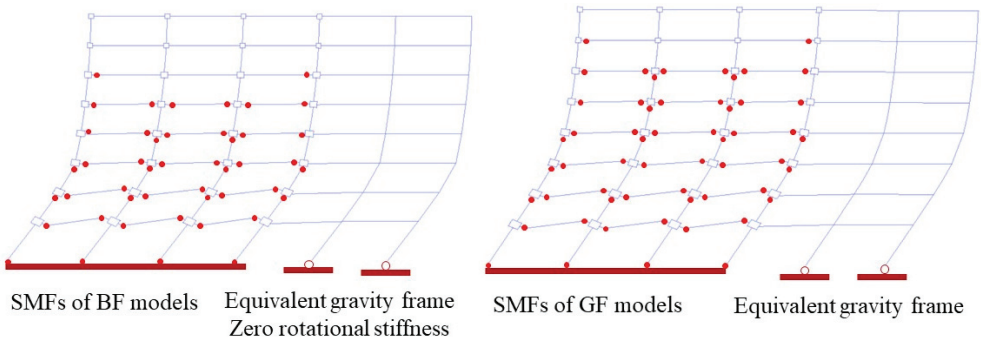


Figure 6 - Collapse mechanisms for the eight story buildings based on different analytical model representations

## 6. NONLINEAR RESPONSE HISTORY ANALYSES AND COLLAPSE RISK

This section quantifies the effect of the gravity framing on the collapse capacity of the steel buildings. The far-field as well as long-distance and strong earthquake ground motion record

sets were selected as defined in FEMA P695 [26] by considering maximum considered earthquake having a 2% probability of being exceeded in 50 years. These sets include 22 component pairs representative of the site and hazard level, for each principal directions (H1, H2) (total of 44 records). Around 2500 nonlinear response history analyses were performed to obtain collapse capacity of the steel buildings through the use of OpenSees software.

The global drift capacity is ultimate building drift capacity against total collapse. Vamvatsikos and Cornell [31] developed incremental dynamic analysis (IDA) procedure to determine global capacity of the building. The ground motions are scaled incrementally based on the IDA. They were also used to capture global trends related to collapse through incremental dynamic analysis.

The procedure that was used to perform IDA is as follows; at first, a linear response history analysis for one of the accelerograms is performed to establish the elastic baseline. The vertical axis of a graph is the 5% damped spectral acceleration at the first mode period of the steel building (calculated in the previous step). Next, a nonlinear response history analysis is performed to obtain maximum inter-story drift value and horizontal axis of the graph is chosen as maximum calculated drift ratio at any story. The slope of the straight line from the origin to this point ( $S_a(T_1, 5\%), \theta_{max}$ ) is referred to elastic slope. Then, the intensity of the ground motion is increased by a scale factor of  $\lambda$  and the analysis is repeated. Note that vertical axis of the IDA curve  $S_a(T_1, 5\%)$  is monotonically increasing with scale factor  $\lambda$ . However, maximum story drift ratio can be deduced from the output of the corresponding detailed non-linear dynamic analysis. The global drift capacity is reached when the building becomes unstable. It occurs when the equivalent stiffness of the building is less than 20% of the slope in the elastic part. This can be thought of as the point at which the inelastic drifts are increasing at 5 times the rate of the elastic drifts. If these conditions do not occur the drift limit of 0.15 is chosen as the global drift capacity. Finally median responses were calculated for the engineering demands calculations. Figure 7 illustrates an example of a single record IDA study of the eight-story steel buildings with SMFs subjected to the North Palm Springs record from the 1992 Landers Earthquake. As seen from the figure, gravity frames could be effective in delaying or preventing dynamic instability.

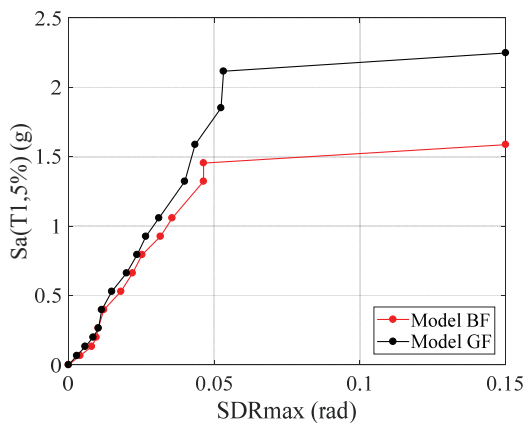
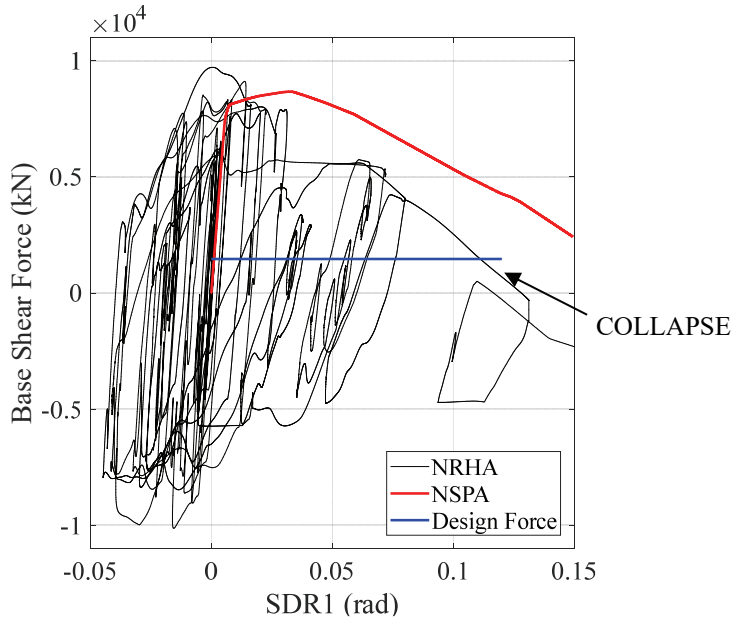


Figure 7 - An example of single record IDA study.

Collapse intensity of the building is defined as the intensity at which a story displaces sufficiently and story shear resistance becomes zero as a result of P-Delta effects accelerated by steel component deterioration in strength and stiffness of the structural components.

Figure 8 illustrates the base shear versus first story drift ratio for the eight story BF model when subjected to the collapse intensity of the North Palm Springs record from the 1992 Landers Earthquake. In the same figure, base shear versus the first story drift ratio from the pushover analysis and base shear design forces have been superimposed. From the figure, it is clear that dynamic over-strength capacity is larger than the static one. This difference is primarily attributed to the dynamic redistribution of story shear forces as a result of higher mode effects. Because NSPA is conducted using the first-mode lateral load pattern only. Therefore, the taller the building, the larger the difference between the static and dynamic base shear. Dynamic over-strength may be noticeable for evaluation of force-sensitive components subjected to earthquake loading.



*Figure 8 - Base shear force versus first story drift ratio curve*

Figure 9 and Figure 10 illustrate the IDA curves including 44 ground motions for the four- and eight-story buildings, respectively in terms of  $S_a(T_1, 5\%)$  versus  $SDR_{max}$ . Each point in the figures corresponds to result of one nonlinear dynamic analysis and each line in the figures connects nonlinear dynamic analysis results from a ground motion record till the collapse of the building.

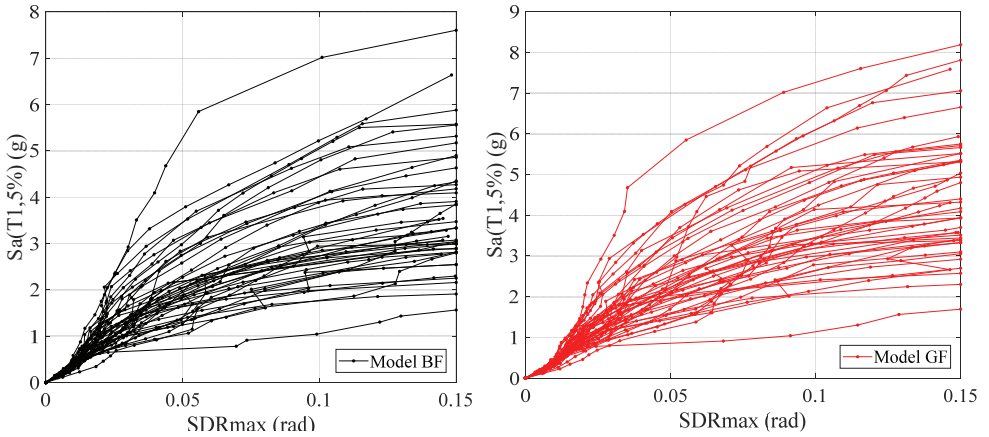


Figure 9 - IDA curves for the four-story buildings

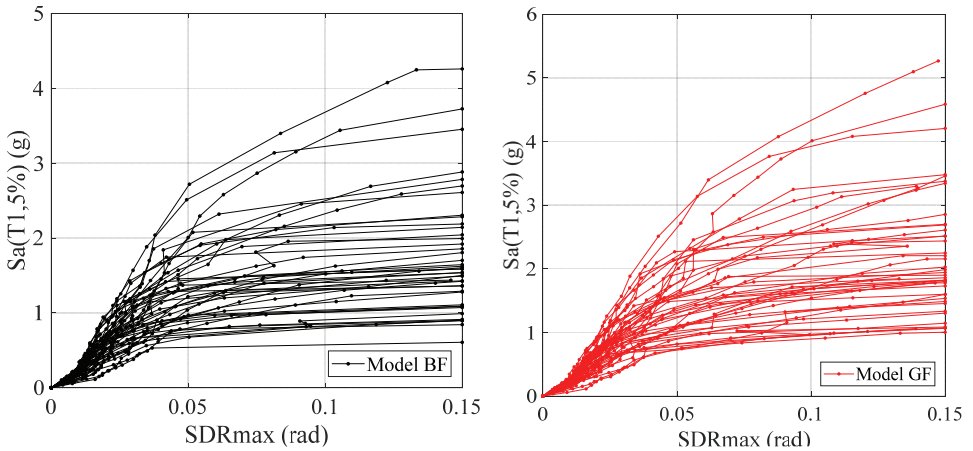


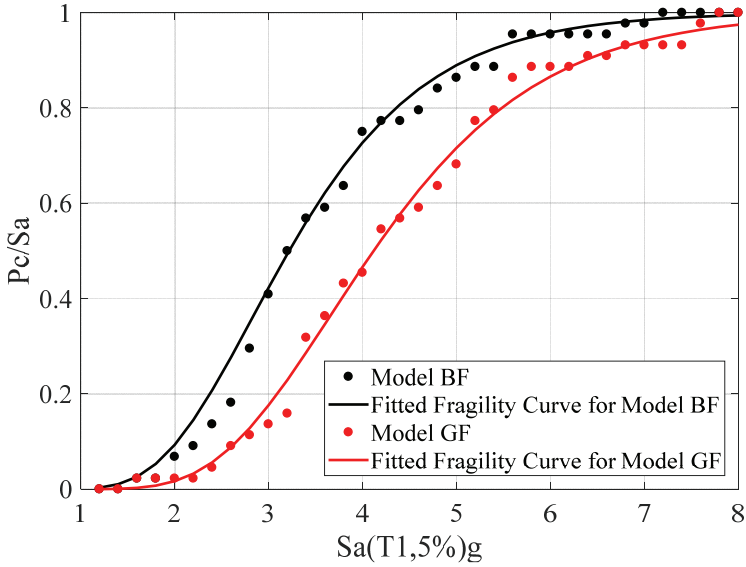
Figure 10 - IDA curves for the eight-story buildings

As seen in these figures, when the gravity framing is considered as a part of the analytical models of the steel buildings, its collapse capacity is larger than the bare BF model. Therefore, collapse probability of the GF model is lower than the bare BF models.

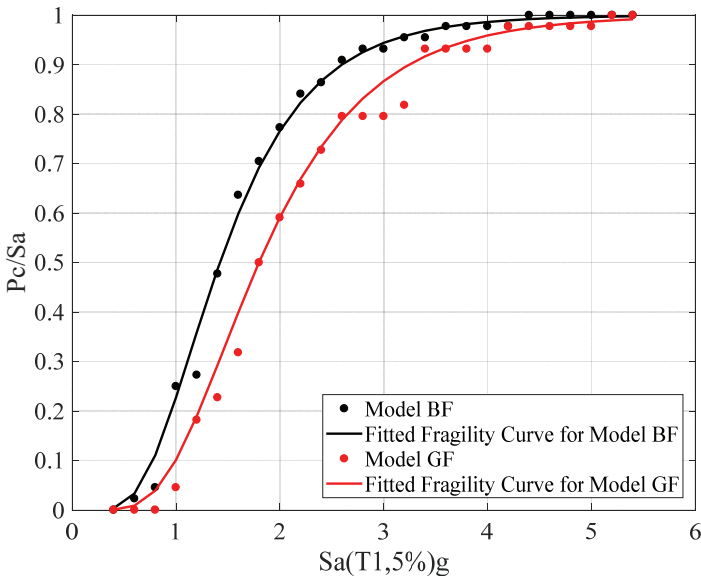
Figure 11 and Figure 12 show the collapse fragility curves for the four-story and eight-story buildings, respectively. The cumulative probabilities of collapse corresponding to 44 collapse intensities obtained from IDAs are calculated and fitted with a lognormal cumulative distribution as shown in the figures.

Table 4 summarizes the median collapse intensity ( $S_{CT}$ ) for the 44 ground motion considered for four-story and eight-story steel buildings. When considering gravity framing, both of the buildings exhibit an average increase about of 27% in the median collapse capacity compared with bare BF models. As a result, according to the FEMA P695 methodology [26], the

collapse margin ratio (CMR), that is the rate of the median collapse intensity of the building to the intensity associated with maximum considered earthquake at the location of the building, is increased.



*Figure 11 - Collapse fragility curves of the four-story steel building*



*Figure 12 - Collapse fragility curves of the eight-story steel building*

Table 4 - Median collapse capacities  $S_{CT}$ , of the four and eight story steel buildings

	$S_{CT}$ (T1, bare 5%) (g)		Global drift capacity	
	4-Story	8-Story	4-Story	8-Story
Model BF	3.218	1.422	0.123	0.083
Model GF	4.117	1.799	0.129	0.106
Model GF / Model BF	1.279	1.265	-	

Compared to four-story buildings, the global drift capacities of the eight-story buildings were reduced as the P-Delta effects are more severe for the eight-story buildings. In case of considering gravity framing, global drift capacities were increased for both of the steel buildings. Similar to NSPA results, global collapse mechanisms involve more stories compared with BF models.

## 7. CONCLUSIONS

In this study, four-story and eight-story buildings with ductile connections, were designed in accordance with Turkish Seismic Code for Buildings 2018. Beam-to-column connections for the interior gravity framing of the buildings were designed as header end-plate connections. In the analysis of structures and particularly in nonlinear dynamic analysis of semi-rigid steel buildings, the connection models should be modelled as realistically as possible. The study presents calibrated hysteretic models based on the experimental data obtained from [14] to represent the actual behavior of header end-plate connections in the GF models, while in the BF models it is idealized as a pin connection. NSPA and NRHAs were performed on steel buildings with SMFs to investigate the effect of gravity framing on structural demands and collapse probability. OpenSees software simulations were conducted. The following conclusions are drawn from this study.

1. The existing rules in TSCB [15] are found to be very strict for the control of SDRs during the design process, leading to overly rigid buildings. To mitigate the requirements of inter-story drift ratio, these rules should be updated. It is suggested to use smaller deflection amplification factor ( $< R/I$ ) to find inter-story drift demand.
2. Steel frame buildings with SMFs, regardless of contribution of gravity framing to lateral strength, have shown to have greater static over-strength factors than code-specified ( $D=3$ ).
3. The period of vibration of the analysed structures decreases when the gravity frame is considered as a part of the structural system. However, since the steel buildings designed in accordance with TSCB 2018 are very rigid, the decrease in the vibration period is small.
4. Dynamic shaking effects caused the engineering demands to change from the static case. As a result of the higher mode effects, the taller the buildings the larger dynamic amplification of story shear forces of the building. Therefore, it is clear that

quantification of demand parameters from NSPA only is questionable for structures that have considerable higher mode effects.

5. Gravity frames can contribute to the mitigation of drift demands by adding lateral stiffness and strength. When considering gravity framing, the base shear strength is 18.5% and 10.8% larger than that of the bare frame only for the four-story and eight-story buildings, respectively. As a result of incremental dynamic analyses, the median collapse intensity of the buildings was average increased about of 27% compared with bare BF models for both of buildings.
6. Models that include the interior gravity frames had smaller drift demands and greater global drift capacity of the buildings than those without them.
7. Bottom story collapse mechanism that is not a desirable scenario for ductile design is triggered when the gravity framing is not regarded as a part of the building during the nonlinear dynamic analyses.
8. The gravity framing system appears to be effective at providing reserve strength and stiffness to the system which helps to prevent or delay collapse.
9. The probability of collapse decreased significantly when the gravity framing is included in the analysis. Incorporation of the gravity framing improved the collapse capacity based on the FEMA P-695 methodology.

## **Symbols**

$BF$	:	Bare frame model
$C_d$	:	Deflection amplification factor
$D$	:	Static over-strength factor
$E$	:	Modulus of Elasticity (N/mm <sup>2</sup> )
$F_y$	:	Nominal yield stress of structural steel
$G$	:	Dead load
$GF$	:	Gravity framing model
$H1, H2$	:	Principle horizontal directions for accelerograms
$I$	:	Importance factor
$I_{b,eq}$	:	Equivalent beam moment of inertia
$I_{b,i}$	:	Moment of inertia of i-th beam in a story
$I_{c,eq}$	:	Equivalent column moment of inertia
$I_{c,i}$	:	Moment of inertia of i-th column in a story
$L_{b,eq}$	:	Equivalent beam length
$L_{b,i}$	:	Length of i-th beam in a story
$MC$	:	Moment resisting connection
$M_p$	:	Flexural strength capacity of bare gravity beam

$M_{p,b,eq}$	: Equivalent beam plastic moment
$M_{pb,i}$	: Plastic Moment of i-th beam in a story
$M_{p,c,eq}$	: Equivalent column plastic moment
$M_{pc,i}$	: Plastic Moment of i-th column in a story
$PC$	: Pin connection
$PC/Sa$	: Probability of collapse for a given intensity $Sa$
$P_{GF}$	: Gravity load for Gravity Frames
$P_{MF}$	: Gravity load for Moment Frames
$Q$	: Live load
$R$	: Response modification factor
$Sa$	: Spectral acceleration
$Sa (T_1, 5\%)$	: 5% damped spectral acceleration at the first mode period of the steel building
$S_{CT}$	Median collapse intensity (g)
$SDR_1$	: First story drift ratio
$SDR_{MAX}$	: Maximum story drift ratio
$S_{DS}$	: Design spectral acceleration at the short period
$S_{D1}$	: Design spectral acceleration at a period of 1 second
$V_{des}$	: Code-based design force of the steel building
$V_{max}$	: Ultimate strength of the steel building
$\theta_{max}$	: Maximum calculated story drift angle
$\lambda$	: Scale factor for the ground motion records
$\mu_T$	: Period based ductility

## Acknowledgments

This research was financially supported by Research Fund of the Istanbul Technical University. Project Number: 41573

## References

- [1] Leon, R., Composite connections, Structural Engineering Handbook, CRC Press LLC, 1999.
- [2] Huang, Z., and Foutch, D.A., Effect of hysteresis type on drift limit for global collapse of moment frame structures under seismic loads, Journal Earthquake Engineering, 13(7), 939-964, 2009.

- [3] Lignos, D., and Krawinkler, H., Sidesway Collapse of Deteriorating Structural systems under Seismic Excitations, Report No. TB 172, John A. Blume Earthquake Engineering Center, Stanford University, CA, 2012.
- [4] Gupta, A., and Krawinkler, H., Behavior of ductile SMRFs at various seismic hazard levels, *Journal of Structural Engineering*, 126(1), 98–107, 2000.
- [5] Ramos, M.D., Mosqueda, G. and Hashemi, M.J., Large-scale hybrid simulation of a steel moment frame building structure through collapse, *Journal of Structural Engineering*, 142(1), 04015086, 2016.
- [6] MacRae, G.A., Kimura, Y. and Roeder, C., Effect of column stiffness on braced frame seismic behavior, *Journal of Structural Engineering*, 130(3), 381-391, 2004.
- [7] Ji, X., Kato, M., Wang, T., Hitaka, T. and Nakashima, M., Effect of gravity columns on mitigation of drift concentration for braced frames, *Journal of Constructional Steel Research*, 65(12), 2148-2156, 2009.
- [8] Elkady, A. and Lignos, D. G., Effect of gravity framing on the overstrength and collapse capacity of steel frame buildings with perimeter special moment frames, *Earthquake Engineering & Structural Dynamics*, 44, 1289-1307, 2015.
- [9] Lee, K. and Foutch, D. A., Performance evaluation of new steel frame buildings for seismic loads, *Earthquake Engineering and Structural Dynamics*, 31, 653-670, 2002.
- [10] Flores, F.X., Charney, F.A. and Lopez-Garcia, D., Influence of the gravity framing system on the collapse performance of special steel moment frames, *Journal of Constructional Steel Research*, 101, 351-362, 2014.
- [11] Foutch, D. A., and Yun, S., Modeling of steel moment frames for seismic loads, *Journal of Constructional Steel Research*, 58, 529-564, 2002.
- [12] Astaneh-Asl, A., Modjtahedi, D., McMullin, K., Shen, J. and D'Amore, E., Stability of damaged steel moment frames in Los Angeles, *Journal of Constructional Steel Research*, 20, 443-446, 1998.
- [13] Sizemore, J., Davaran, A., Fahnestock, L., Tremblay, R. and Hines, E., Seismic behaviour of low-ductility concentrically-braced frames, *Structures Congress, ASCE Library*, 2014.
- [14] Karasu, A. and Vatansver, C., Experimental Study on the Behavior of Header End - Plate Connections under Cyclic Loading, *Technical Journal of Turkish Chamber of civil engineers*, 32(6), 2021.
- [15] Turkish Seismic Code for Buildings 2018, Specifications for Design of Buildings under Earthquake Action, Disaster and Emergency Management Presidency, Ankara.
- [16] Chisari, C., Francavilla, A.B., Latour, M., Piluso, V., Amadio, C. and Rizzano, G., Critical issues in parameter calibration of cyclic models for steel members, *Engineering Structures*, 132, 123-138, 2017.
- [17] OpenSees, Version 2.0, User Command-Language Manual, 2009.

- [18] Turkish code for design and construction of steel structures 2016, Ministry of Environment and Urbanisation, Ankara, Turkey.
- [19] Krawinkler, H., The state-of-the-art report on system performance of moment resisting steel frames subjected to earthquake ground shaking, FEMA 355c, Washington, DC: Federal Emergency Management Agency, 2000.
- [20] CSI. SAP2000 v18 integrated finite element analysis and design of structures, Berkeley: Computers and Structures; 2016.
- [21] Ibarra, L.F., Medina, R.A., and Krawinkler, H., Hysteretic models that incorporate strength and stiffness deterioration, *Earthquake Engineering Structural Dynamic*, 34(12), 1489-1511, 2005.
- [22] Lignos, D. G. and Krawinkler, H., Deterioration Modeling of Steel Components in Support of Collapse Prediction of Steel Moment Frames under Earthquake Loading, *Journal of Structural Engineering*, 137 (11), 1291-1302, 2011.
- [23] Lignos, D. G., Hartloper, R.H., Elkady, A., Deierlein, G.G. and Hamburger, R., Proposed Updates to the ASCE 41 Nonlinear modeling parameters for wide-flange steel columns in support of performance-based seismic engineering, *Journal of Structural Engineering*, 145 (9), 04019083, 2019.
- [24] Gupta, A. and Krawinkler, H., Seismic demands for the performance evaluation of steel moment resisting frame structures, Report No. 132, The John A. Blume Earthquake Engineering Center, Stanford University, CA, 1999.
- [25] Lignos, D.G., Putman, C., Krawinkler, H., Seismic assessment of steel moment frames using simplified nonlinear models, *Computational Methods in Earthquake Engineering*, 30(0), 91–109, 2013.
- [26] FEMA, Quantification of building seismic performance factors, Report FEMA-P695, Federal Emergency Management Agency, Washington, DC, 2009.
- [27] Zareian, F., Medina, R.A., A practical method for proper modeling of structural damping in inelastic plane structural systems, *Computers & Structures*, 88(1), 45–53, 2010.
- [28] Chopra, A.K., *Dynamics of structures theory and applications to earthquake engineering*, Fourth edition, Prentice Hall, U.S.A, 2013.
- [29] Lignos, D.G., Putman, C., Krawinkler, H., Application of simplified analysis procedures for performance-based earthquake evaluation of steel special moment frames, *Earthquake Spectra*, 31(4), 2015.
- [30] ASCE/SEI 7-16, Minimum design loads for buildings and other structures, Reston, VA: ASCE, 2017.
- [31] Vamvatsikos, D., Cornell, C.A., Incremental dynamic analysis, *Earthquake Engineering & Structural Dynamics*, 31(3), 491–514, 2002.

